ORIGINAL ARTICLE

Effect of murine double-minute 2 inhibitors in preclinical models of advanced clear cell carcinomas originating from ovaries and kidneys

Yoshiko Kawata[1] | Kazunori Nagasaka[1,2] (iD) | Katsutoshi Oda[1] | Chinami Makii[1] |
Makoto Takeuchi[1] | Shinya Oki[1] | Harunori Honjo[1] | Machiko Kojima[1] |
Yuko Miyagawa[2] | Ayumi Taguchi[1] | Michihiro Tanikawa[1] | Kenbun Sone[1] |
Haruko Hiraike[2] | Yoko Matsumoto[1] | Osamu Wada-Hiraike[1] | Takuya Ayabe[2] |
Yutaka Osuga[1] | Tomoyuki Fujii[1]

[1]Department of Obstetrics and Gynecology, Graduate School of Medicine, The University of Tokyo, Tokyo, Japan

[2]Department of Obstetrics and Gynecology, Teikyo University School of Medicine, Tokyo, Japan

Correspondence
Kazunori Nagasaka, Department of Obstetrics and Gynecology, Teikyo University School of Medicine, Tokyo, Japan.
Email: nagasakak-tky@umin.ac.jp

Funding information
Grant-in-Aid for Scientific Research C, Grant/Award Number: 15K10705, 19K09834 and 18K09249; the Project for Cancer Research and Therapeutic Evolution (P-CREATE); P-CREATE

Abstract

Advanced clear cell carcinomas originating from both ovaries and kidneys with cancerous peritonitis have poor prognoses. Murine double-minute 2 (MDM2) is a potential therapeutic target for clear cell ovarian carcinomas with WT *TP53*. Herein, we characterized the antiangiogenic and antitumor effects of the MDM2 inhibitors DS-3032b and DS-5272 in 6 clear cell ovarian carcinoma cell lines and 2 clear cell renal carcinoma cell lines, as well as in clear cell ovarian carcinomas s.c. xenograft and ID8 (murine ovarian cancer cells with WT *TP53*) cancer peritonitis mouse models. In clear cell ovarian carcinoma s.c. xenograft mouse models, DS-3032b significantly reduced WT *TP53* clear cell ovarian carcinoma- and clear cell renal carcinoma-derived tumor volumes. In ID8 mouse models, DS-5272 significantly inhibited ascites production, reduced body weight, and significantly improved overall survival. Additionally, DS-5272 reduced the tumor burden of peritoneal dissemination and decreased CD31^{+} cells in a dose-dependent manner. Furthermore, DS-5272 significantly decreased vascular endothelial growth factor concentrations in both sera and ascites. Combined therapy with MDM2 inhibitors and everolimus showed synergistic, and dose-reduction potential, for clear cell carcinoma treatment. Our findings suggest that MDM2 inhibitors represent promising molecular targeted therapy for clear cell carcinomas, thereby warranting further studies to evaluate the efficacy and safety of dual MDM2/mTOR inhibitors in clear cell carcinoma patients.

1 | INTRODUCTION

Murine double-minute 2 is an E3 ubiquitin ligase that binds to and degrades p53 through proteasomes following polyubiquitination.[1,2] Furthermore, MDM2 is a negative regulator of the _TP53_ tumor-suppressor gene and acts by inhibiting _TP53_ transcriptional activity and its translocation from the nucleus to the cytoplasm.[3] More than 17% of tumors in humans show _MDM2_ amplification, which leads to poor prognosis and treatment failure with present-day chemotherapeutics. Additionally, ~50% of all cancers retain WT p53, wherein the p53 pathway is inactivated by the overexpression of endogenous negative regulators. In particular, _MDM2_ amplification occurs in ~7% of all human cancers without concomitant _TP53_ mutation.

Recently, we showed that high levels of MDM2 in CCOC were negatively correlated with PFS and OS and an independent factor associated with poor prognoses.[4] Unlike early stage, advanced stage CCOC patients can develop deep vein thrombosis, pulmonary embolisms, peritoneal dissemination, and massive hemorrhagic ascites in the peritoneal cavity, with ascites development influencing the poor prognosis.[5] In such cases, standard chemotherapy becomes insufficient due to these clinical complications.[6] Effective alternative treatments have not been identified, and as such, the establishment of molecular-targeting therapy focused on advanced CCOC is warranted.

Clear cell renal carcinoma accounts for ~80% of renal cell carcinomas and has histopathological and molecular biological similarities to CCOC[7]; however, gene mutations in CCRC include a high frequency of inactivating mutations in the Von Hippel–Lindau tumor-suppressor gene (_VHL_) and only a low frequency of PI3K/Akt/mTOR pathway and _TP53_ mutations. Nevertheless, similar to CCOC, MDM2 levels are significantly correlated with PFS and OS in CCRC, and its high expression is reportedly an independent poor prognostic factor.[8,9]

Thus, _MDM2_ overexpression has been associated with increased metastasis and advanced disease in several cancers.[10] Given the link between poor outcomes and p53 and MDM2 levels, blocking the MDM2-p53 interaction is expected to be a reasonable therapeutic target for various advanced cancers.[11] The MDM2-p53 binding inhibitors show antitumor effects both in vivo and in vitro in cancers with WT _TP53_.[11] MDM2 and p53 interact at their first 120 and first 30 N-terminal amino acid residues, respectively, through 3 key binding residues, Phe19, Trp23, and Leu26.[12] Inhibitors, such as Nutlin-3a and RG-7112, mimic the 3-D structure of these 3 residues, with RG-7112 capable of inducing apoptosis in CCOC through activation of p53.[13] These results suggest that reactivating p53 could prove to be a promising therapeutic strategy for tumors expressing WT p53. Additionally, MDM2 reportedly increases the gene expression of hypoxia-inducible factor-1 (_HIF-1_) and _VEGF_.[14,15] Moreover, the detachment and adhesion of cancer cells is strongly related to

angiogenesis[16]; therefore, we investigated the antitumor effects and inhibition of ascites by an MDM2 inhibitor that also exerts an inhibitory effect on VEGF activity in a WT _TP53_ CCOC cell line.

The PI3K/Akt/mTOR signaling pathway, which in turn activates MDM2, is frequently triggered in cancers.[17-21] Additionally, the mTOR inhibitors everolimus and temsirolimus have been used clinically to treat renal cell carcinoma, neuroendocrine tumors, breast cancer, and tuberous sclerosis.[22,23] In noncancerous cells, p53 suppresses the PI3K/Akt signaling pathway by activating PTEN,[24] and Akt can directly phosphorylate and stabilize MDM2 and promote p53 degradation.[25,26] However, _PTEN_ mutations are only observed in 5% of CCOC cases,[21] suggesting that the mTOR signaling pathway and the MDM2 pathway are mutually affected in CCOC. Interestingly, the PI3K/mTOR coinhibitor DS-7423 shows an antitumor effect against CCOC and a synergistic effect in combination with the aforementioned MDM2 inhibitor RG-7112.[4,14,20]

_TP53_ mutations occur in less than 10% of CCOC cases.[27] Furthermore, mutations in _PIK3CA_, which activates the PI3K/Akt/mTOR pathway, are found in ~40% of CCOC cases, human epidermal growth factor receptor 2 gene (_HER2_) overexpression occurs in ~30%, and _cMET_ is overexpressed in ~30% along with frequent activation of receptor tyrosine kinase.[21,28] Based on this molecular biological background, the mTOR pathway is considered a promising therapeutic target against CCOC.

In the present study, we preclinically evaluated the antitumor effect of the MDM2 inhibitors DS-5272[29] and DS-3032b,[30] as well as their ability to suppress ascites formation, on _TP53_ WT CCOC and CCRC. DS-3032b is currently in phase I clinical trials for relapsed acute myeloid leukemia (NCT02319369) and advanced solid tumors or lymphomas (NCT01877382). Additionally, we examined the in vivo and in vitro antitumor effects of their combination use of the MDM2 inhibitors with everolimus in CCCs originating from ovaries and kidneys.

2 | MATERIALS AND METHODS

2.1 | Ethics approval and consent to participate

The study was carried out in accordance with the Declaration of Helsinki. This study was approved by the Animal Care and Use Committee of the University of Tokyo. Athymic mice were maintained in a specific pathogen-free facility according to our institutional guidelines, and experiments were undertaken according to an approved animal care protocol (P13-121). In the study, the allocation process was carried out by random selection without any other criteria.

Specific pathogen-free female nude mice (BALB/cAJc1-nu/nu) and C57/BL6 female mice were used in the study. Five-week-old BALB/

cAJc1-nu/nu mice and 8-week-old C57/BL6 female mice were housed in groups of 5 per cage and subjected to treatment under specific pathogen-free conditions in the section of the clinical research center at the University of Tokyo according to approved protocols and guidelines of the Institutional Animal Care and Use Committee. The animals were kept under controlled environmental conditions ($23 \pm 1°C$; 12/12 h night-day cycle) with ad libitum access to food and water. Zeitgeber 0 was at 8:00 AM. The mean body weight of all mice was approximately 21-22 g. All mice were naïve to previous drug treatments. All animals were randomly divided into 3 groups (n = 7-8/group) for the study.

2.2 | Tumor xenografts in nude mice

Specific pathogen-free female nude mice (BALB/cAJc1-nu/nu) were purchased from CLEA Japan (Tokyo, Japan). Nude mice bearing OVISE, Caki-1, or ES-2 tumor xenografts were established, as follows: OVISE, Caki-1, or ES-2 cells (2×10^7) were injected s.c. using 27-G needle into the 5-week-old mice, and the s.c. implanted tumor was allowed to grow to 5 mm in diameter. The mice were then randomly assigned to 3 groups (n = 7-8/group), and each mouse was treated daily for 3 weeks with either an oral dose of 50 mg/kg or 100 mg/kg DS-3032b or vehicle, or DS-3032b (50 mg/kg) and everolimus (5 mg/kg). Mice were weighed over time, and the tumor size and body weight of the xenograft mouse models were measured after the start of treatment. At the termination of treatment, all mice were anesthetized with 4% isoflurane (Fujifilm Wako, Tokyo, Japan) in 100% oxygen until loss of righting reflex and killed by cervical dislocation. Tumor volume was calculated according to the following formula: ([major axis] × [minor axis]^2) / 2. Tumors were collected from mice killed after 21 days of treatment, and tumor weights were compared between treated animals and controls using t tests.

2.3 | Cancer peritonitis mouse model

C57/BL6 mice were purchased from Japan SLC, and ID8 cells (2×10^6) in PBS were introduced into the mice by i.p. injection using a Hamilton syringe (27-G needle). After 7 weeks, the mice were randomly assigned to 3 groups (n = 7-8/group) and received daily oral treatment with 25, 50, or 100 mg/kg of DS-5272 or vehicle for 4 weeks. ID8 mice were monitored twice every other day. At the termination of treatment, all mice were anesthetized with isoflurane, and killed. After mice were killed, blood and ascites were collected and analyzed. Peritoneal seeding that formed on the visceral peritoneum of the anterior abdomen was removed, along with the abdominal wall, and analyzed. Group means were compared by paired t tests.

2.4 | Cell lines and compounds

We used 6 human CCOC cell lines (OVISE, OVTOKO, JHOC-7, JHOC-9, ES-2, and SKOV-3), 2 CCRC cell lines (Caki-1 and Caki-2),

and 1 mouse ovarian carcinoma cell line (ID8). The OVISE and OVTOKO cell lines were purchased from the Japanese Collection of Research Bioresources Cell Bank. JHOC-7 and JHOC-9 cell lines were purchased from the RIKEN Cell Bank. ES-2, SKOV3, Caki-1, and Caki-2 cell lines were purchased from ATCC. ID8 cells were kindly gifted by Dr Kathy Roby of the Department of Anatomy and Cell Biology at the University of Kansas Medical Center. All cell lines were cultured at 37°C in a humidified incubator with 5% CO_2. All 9 cell lines were classified histologically as CCCs and authenticated by short tandem repeat analysis. We used the International Cell Line Authentication Committee database to confirm that these cell lines were not cross-contaminated or misidentified. The MDM2 inhibitors DS-3032b and DS-5272 were provided by the Daiichi-Sankyo Company, and the mTOR inhibitor everolimus was purchased from LC Laboratories.

2.5 | Cell proliferation assays

Cells were seeded in 96-well plates (2×10^3 cells/well), and after 24 hours, the medium was replaced with fresh medium containing various concentrations of DS-3032b, DS-5272, and/or everolimus. Cell viability was normalized to cells treated with 0.4% DMSO. After 72 hours, CCK-8 solution (50 μL; Dojindo) was added to each well. Proliferation was quantified by monitoring changes in absorbance at 450 nm using a microplate reader (BioTek).

2.6 | Cell cycle analysis

Cells were seeded in 60-mm dishes (2×10^5 cells/dish). After 24 hours of incubation, the medium was replaced with fresh medium containing various concentrations of DS-3032b, DS-5272, and/or everolimus and incubated for 48 hours. Cells were collected using trypsin and stained in the dark with 50 μg/mL PI (Sigma-Aldrich) at 4°C for 30 minutes. Cell-cycle distribution was analyzed by flow cytometry on an Epics XL instrument (Beckman Coulter) using Cell Quest Pro software (version 3.1; BD Bioscience).

2.7 | Detection of apoptosis

Cells were seeded in 6-well plates (2×10^5 cells/well). After 24 hours of incubation, the medium was replaced with fresh medium containing DS-3032b, DS-5272, and/or everolimus and incubated for 48 hours. Cells were collected using trypsin and washed twice with PBS. Collected cells were resuspended in 1× binding buffer and stained with FITC-conjugated annexin V/PI (annexin V-FITC apoptosis detection kit II; BD Biosciences) in the dark for 15 minutes. Annexin V-FITC/PI double-positive cells were detected by flow cytometry and expressed as a percentage of apoptotic cells.

2.8 | Western blot analysis

Equivalent amounts of lysate protein (10 μg) were subjected to Mini-PROTEAN TGX precast protein gels (Bio-Rad) and electrophoretically transferred onto Trans-Blot Turbo transfer packs (Bio-Rad) using the Trans-Blot Turbo transfer system (Bio-Rad). After blocking, the membranes were incubated overnight at 4°C with the primary Abs anti-MDM2 (1:1000, sc-56154), anti-p53 (1:1000, sc-53394), and anti-p21 (1:1000, sc-6246) purchased from Santa Cruz Biotechnology, mouse anti-p53 (1:200, ab26; Abcam), anti-phospho-TP53 (Ser15; 1:500, 9286S), anti-cleaved PARP (1:1000; 5625S), anticleaved caspase 3 (1:1000, 9664P), and anti-PUMA (1:1000, 4976S), anti-S6 (1:1000, 2217), anti-4EBP1 (1:1000; 9644), anti-phospho-S6 (1:1000, 5364), anti-phospho-4EBP1 (1:1000, 2855) obtained from Cell Signaling Technology, anti-survivin (1:1000, 332; Novus Biologicals), and anti-β-actin (1:10 000, AC74; Sigma-Aldrich). The blots were then incubated with the appropriate secondary Abs (anti-rabbit IgG [7074S, 1:2000] or anti-mouse IgG [7076S, 1:2000] purchased from Cell Signaling Technology) at room temperature for 1 hour. Protein signals were visualized with the enhanced chemiluminescence select western blotting detection kit (GE Healthcare Life Sciences), and the images were scanned using a luminescent image analyzer (Image Quant LAS 4000 mini; GE Healthcare). The expression of target proteins was internally normalized to the optical density of β-actin (1:2000, A2228; Sigma-Aldrich) using ImageJ software (NIH).

2.9 | Colony formation assay

Cells were seeded in 6-well plates (1 × 10^3 cells/well), and after 24 hours of incubation, the medium was replaced with fresh medium containing various concentrations of DS-5272 or 0.1% DMSO, followed by 7 days of incubation. The cells were fixed with 100% methanol for 5 minutes and stained with Giemsa (Wako) for 30 minutes.

2.10 | Cell apoptosis assay

Tissue sections collected from mice were fixed in 4% paraformaldehyde for 15 minutes at room temperature. After an endogenous
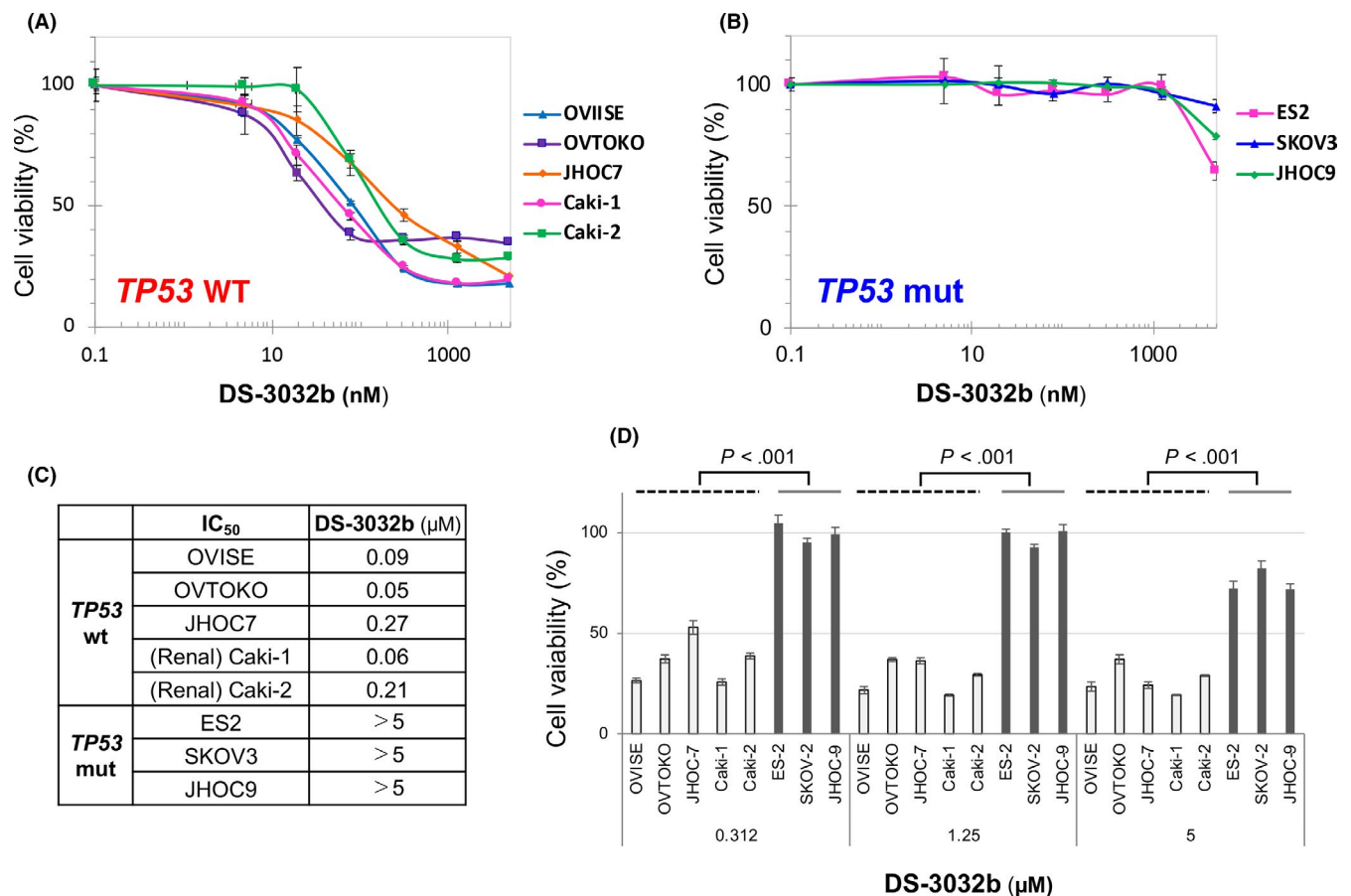
FIGURE 1 Cell viability in clear cell carcinomas (CCCs) treated with DS-3032b. A, B, Cell viability, as measured by MTT assay, in cells with (A) WT or (B) mutant (mut) *TP53*. After treatment with various concentrations of DS-3032b (4.9-5000 nmol/L) for 72 h, 8 CCC cell lines were subjected to a cell viability assay. Cell viability (%) was normalized to cells treated with 0.5% DMSO. C, IC$_{50}$ values for DS-3032b in 8 CCC cell lines. D, Differences in cell viability in cell lines with WT or mutant *TP53* exposed to the indicated concentrations of DS-3032b. Group means were compared by paired *t* test

peroxidase block in H_2O_2 methanol, the sections were incubated on ice for 5 minutes with permeabilization buffer (MK505; TaKaRa Bio) and then treated with TdT enzyme (MK502; TaKaRa Bio) and Labeling Safe buffer (MK502; TaKaRa Bio) for 60 minutes at 37°C, followed by treatment with anti-FITC HRP conjugate (MK503; TaKaRa Bio) for 30 minutes at 37°C. Tumors were stained with 3,3-diaminobenzidine (Dako) and hematoxylin (Wako).

2.11 | Immunohistochemistry for CD31

Tumor sections were fixed in 4% paraformaldehyde at 4°C for 10 minutes, immersed in 1% H_2O_2 at room temperature for 30 minutes to quench endogenous peroxidases, and blocked at room temperature for 30 minutes with Blocking One (Nacalai Tesque). Sections were then probed at 4°C overnight with 1:500 anti-CD31 (PECAM-1; BD Biosciences), washed in TBS, labeled at room temperature for 45 minutes with 1:400 biotinylated rabbit anti-rat (Dako), and then labeled at room temperature for 45 minutes with streptavidin-biotin (Dako). Sections were stained with 3,3-diaminobenzidine and hematoxylin. Harvested s.c. tumors were immunostained with anti-mouse CD31 (PECAM-1; BD Biosciences). The

number of stained microvessels was counted at 400× in 4 random fields for each tumor.

2.12 | Enzyme-linked immunosorbent assay

Blood samples were collected by jugular vein puncture before the mice were killed. After the mice were killed, the VEGF concentrations in the ascites and sera were measured using a mouse VEGF Quantikine ELISA kit (MMV00; R&D Systems) according to the manufacturer's instructions.

2.13 | Statistical analysis

Statistical analysis of in vitro and in vivo assays was carried out using t tests. The definition CI was calculated by the Chou-Talalay method with CI < 1, CI = 1, and CI > 1 representing a synergistic, additive, and antagonistic effect, respectively. In all tests, differences were considered to be significant at $P < .05$. We compared the 4 compound groups (vehicle, DS-3032b, everolimus, and DS-3032b + everolimus) in the xenograft studies using 2-way ANOVA.
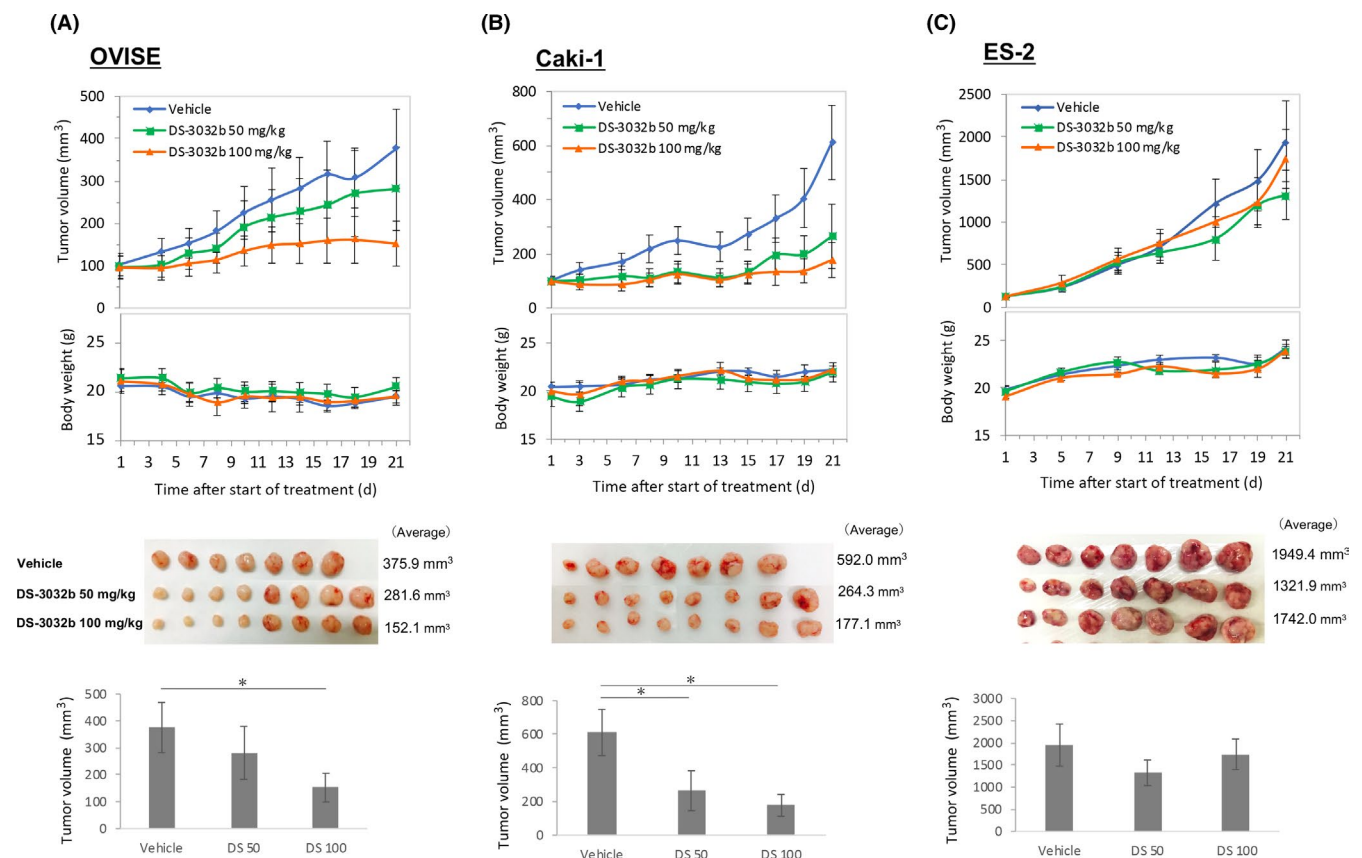
FIGURE 2 In vivo evaluation of DS-3032b efficacy using xenografted OVISE, Caki-1, and ES2 cells. A-C, OVISE (A), Caki-1 (B), and ES-2 (C) cells were injected s.c. into female BALB/cAJc1-nu/nu nude mice. The mice received a daily oral dose of DS-3032b for 3 weeks (n = 7-8/group). Tumor size and body weight of xenograft mouse models treated with DS-3032b were measured after the start of DS-3032b treatment. Tumors were collected from mice after 21 days of DS-3032b treatment. Tumor weights were compared between control and DS-3032b-treated animals using t tests

3 | RESULTS

3.1 | Antitumor effect of DS-3032b in CCCs with WT *TP53*

The antiproliferative effect of DS-3032b, an MDM2 inhibitor, was evaluated in 4 WT (OVISE, OVTOKO, JHOC7, Caki-1, and Caki-2) and 3 mutated (SKOV3, JHOC-9, and ES-2) CCC cell lines. DS-3032b only suppressed cell proliferation in a dose-dependent fashion in WT *TP53* lines, with an IC_{50} range of 0.05 to 0.27 μmol/L (Figure 1A,C). By contrast, the IC_{50} was greater than 5 μmol/L in cell lines with mutant *TP53* (Figure 1B,C). Additionally, cell viability differed significantly between tumors from WT and mutated *TP53* cell lines ($P < .001$ by paired t test; Figure 1D). Western blot indicated that DS-3032b increased levels of MDM2, p53, and p21 in WT-*TP53* OVISE cells in a time- and concentration-dependent manner (Figure S1A,B). The p53 residue, Ser15, is the primary target of the DNA-damage response and is phosphorylated by both ATM and ATR protein kinases, and the results in Figure S1A showed that Ser15 phosphorylation is required for p53 function induced by MDM2 inhibition. Moreover, MDM2 inhibition resulted in the upregulation of p53, p21, and PUMA levels

after DS-3032b treatment. Furthermore, levels of survivin, an antiapoptosis factor, were dramatically suppressed, whereas those of cleaved PARP and cleaved caspase-3 were enhanced by MDM2 inhibition (Figure S1B). The WT *TP53* cells OVISE (a CCOC cell line) and Caki-1 (a CCRC cell line) both showed increased p53, cleaved PARP, and cleaved caspase-3 levels in response to DS-3032b treatment, whereas these protein levels were not increased in the mutant *TP53* cell line ES-2 (Figure S1B,C).

To further examine whether the activation of p53 is associated with DS-3032b-induced cell death, we analyzed the cell-cycle distribution of CCCs (OVISE and Caki-1) with WT *TP53* by fluorescence-activated cell sorting after 48 hours of exposure to DS-3032b. The proportion of cells in sub-G_1 increased to between 12% and 59% following treatment with 0.1 or 1 μmol/L DS-3032b, whereas the S phase population diminished (Figure S1D). Double staining with annexin V and PI indicated that the addition of 0.1 or 1 μmol/L DS-3032b to OVISE and Caki-1 cells significantly increased the ratio of apoptotic cells by 13% to 18% (Figure S1E).

To examine the antitumor activity of DS-3032b in vivo, we established s.c. tumor xenograft models in 5-week-old nude mice with OVISE, Caki-1, or ES-2 cells. At 50 mg/kg, DS-3032b began
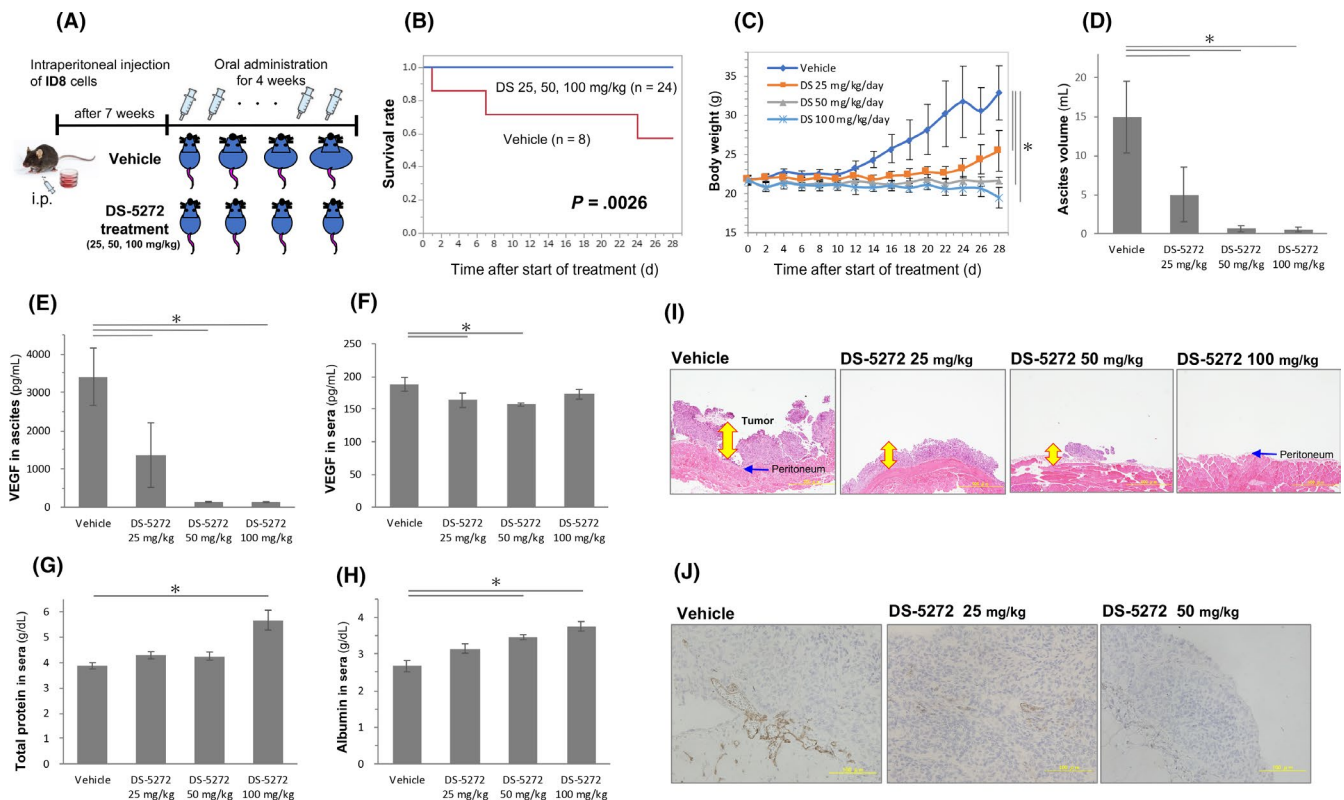
FIGURE 3 In vivo evaluation of DS-5272 efficacy using the ID8 cancer peritonitis mouse model. A, ID8 cells were injected i.p. into C57/BL6 mice. After 7 weeks, the mice received a daily oral dose of DS-5272 for 4 weeks (n = 7-8/group). B, Kaplan-Meier curves. C, D, Effects of DS-5272 on ascites were analyzed by measuring body weight (C) and ascites volume (D) of mice. Means were compared by paired t test. *$P < .05$. E, F, Antiangiogenic effects of DS-5272 evaluated by determining vascular endothelial growth factor (VEGF) concentration in ascites (E) and sera (F) of ascites. Error bars represent mean ± SD. Statistical significance was determined by Student's t test. *$P < .05$. G, H, Total protein (G) and albumin (H) levels in sera. Error bars represent mean ± SEM. Statistical significance was determined by Student's t test. *$P < .05$. I, Histologic examination of the visceral peritoneum of mice by H&E staining. J, Immunohistochemical staining of CD31 to detect microvessels in ID8 peritoneal dissemination from control and DS-5272-treated mice

to suppress the growth of xenografted OVISE and Caki-1 cells, with this suppression becoming significant at 100 mg/kg ($P < .005$; Figure 2A,B). By contrast, DS-3032b did not inhibit tumor growth in xenografted ES-2 cells (Figure 2C). No distinct adverse events were observed with any of the experimental protocols during drug treatment, and no weight loss of more than 10% of initial body weight was observed. No signs of toxicity were observed in the treated mice during the follow-up examinations.

3.2 | Ascites inhibition and antitumor effect of DS-5272 in the WT *TP53* ID8 ovarian cancer model

In the mouse ovarian cancer cell line ID8, a colorimetric assay indicated that DS-5272 inhibited cell proliferation in a concentration-dependent manner, with an IC_{50} of 0.68 μmol/L (Figure S2A), and a colony formation assay subsequently confirmed cell growth inhibition (Figure S2B). Flow cytometry of ID8 cells after 48 hours of exposure to DS-5272 revealed an increase in the sub-G_1 population and a shortened S phase (Figure S2C). Moreover, western blot analysis confirmed that DS-5272 increased MDM2 and p53 levels

in a concentration-dependent manner (Figure S2D). To examine the ability of DS-5272 in improving prognosis and inhibiting ascites in vivo, a cancerous ascites mouse model was created using the ID8 cell line (Figure 3A). No cell deaths were observed in the DS-5272 group, and an apparent prolonging of survival was observed when comparing this group with the vehicle group according to the log-rank Kaplan-Meier method ($P = .0026$; Figure 3B). Furthermore, DS-5272 significantly inhibited ascites in a concentration-dependent manner ($P < .005$; Figure 3C,D).

Additionally, VEGF production in ascites was suppressed by DS-5272 in a concentration-dependent manner (Figure 3E), whereas the decrease in serum VEGF levels was not significant among 25, 50, and 100 mg/kg DS-5272 (Figure 3F). We found that DS-5272 increased both total protein and albumin levels; however, although albumin levels increased significantly following treatment with both 50 and 100 mg/kg DS-5272, total protein levels only increased significantly at a dose of 100 mg/kg ($P < .005$; Figure 3G,H). Moreover, DS-5272 suppressed the formation of peritoneal seeding in a concentration-dependent manner (Figure 3I), with CD31 staining of peritoneal seeding confirming the inhibitory effect of DS-5272 on angiogenesis (Figure 3J).
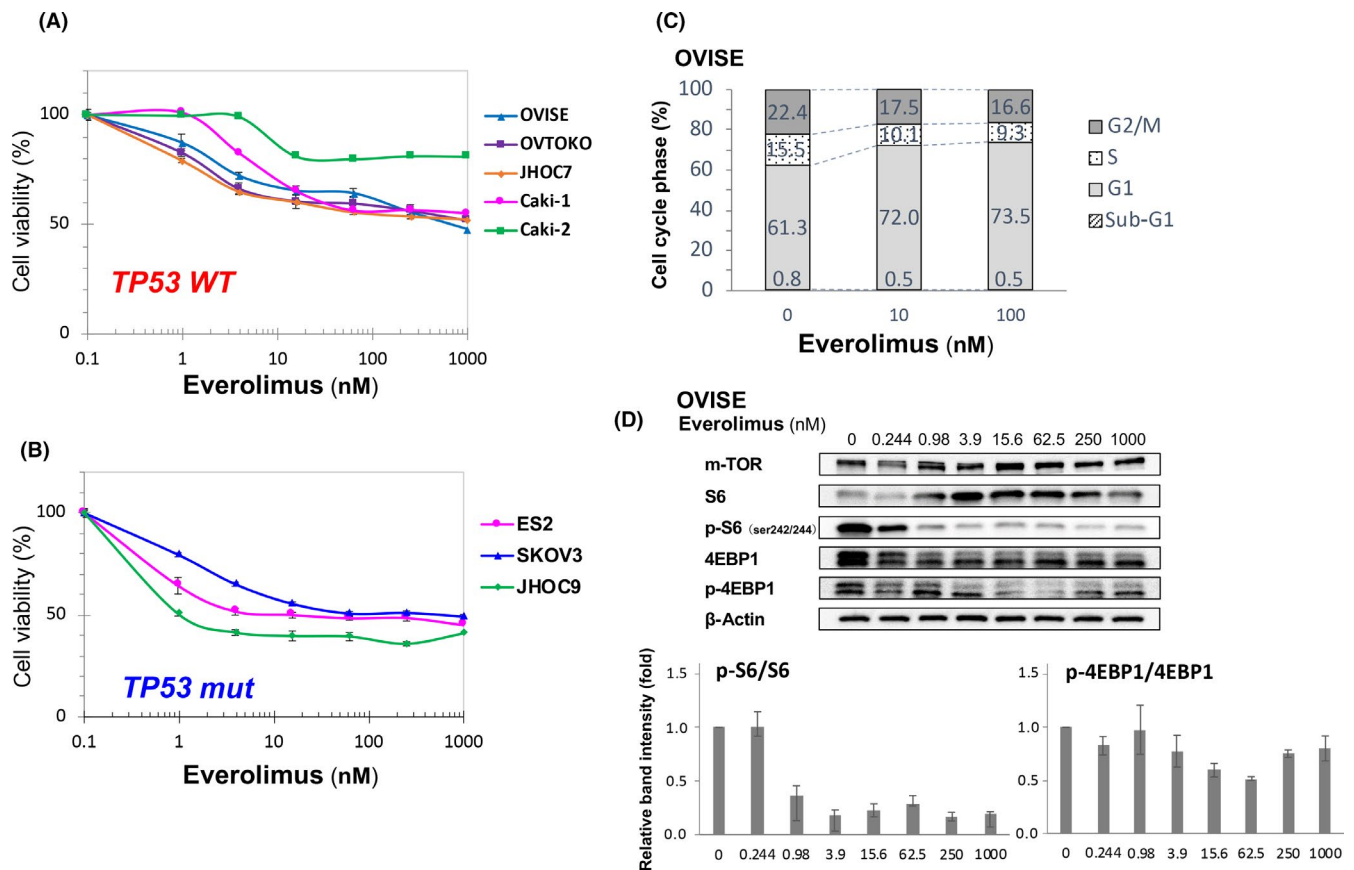
FIGURE 4 Cell viability, cell cycle status, and expression of mTOR target proteins in clear cell carcinomas treated with everolimus. A, B, Cell viability, as measured by an MTT assay, in cells with WT (A) or mutant (mut) (B) *TP53* after treatment with various concentrations of everolimus (0.32-1000 nmol/L) for 72 h. Cell viability (%) was normalized to cells treated with 0.1% DMSO. C, OVISE cells were treated with 10 nmol/L and 100 nmol/L everolimus or 0.1% DMSO for 4 h. Cell cycle status was analyzed by flow cytometry and propidium iodide staining. D, Western blot analysis of mTOR target proteins in OVISE cells after treatment with various concentrations of everolimus (0.244-1000 nmol/L) or 0.01% DMSO for 4 h

3.3 | Antitumor effect of combined DS-3032b and mTOR inhibitor therapy against CCCs with WT *TP53*

We then evaluated the antiproliferative effect of dual inhibition of MDM2 (by DS-3032b) and mTOR (by everolimus) using 5 WT *TP53* cell lines (CCOC cell lines OVISE, OVTOKO, and JHOC7 and CCRC cell lines Caki-1 and Caki-2), as well as the *TP53* mutant cell line SKOV-3. The evaluation of the effects of everolimus alone by colorimetric assays confirmed its inhibitory effect on cell growth, which was ~50% for both WT *TP53* and mutant cell lines (Figure 4A,B). The effect of everolimus on the cell cycle of OVISE cells after 48 hours of exposure showed an increased proportion of cells in the G_1 phase, but no increase in the sub-G_1 population (Figure 4C). Furthermore, western blot analysis of the effect of everolimus on PI3K/Akt/mTOR signaling showed decreased phospho-S6 and phospho-4EPP1 levels (Figure 4D).
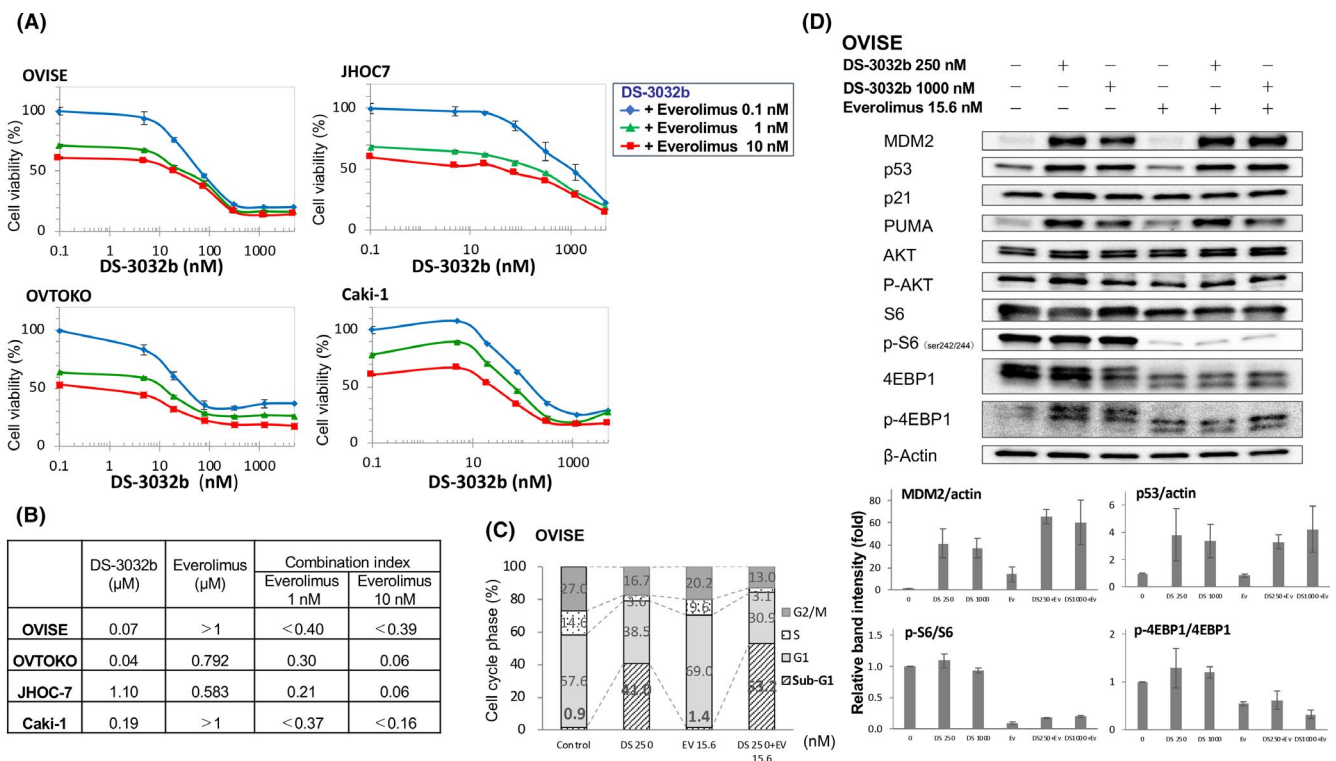
Combined treatment with DS-3032b (4.9-5000 nmol/L) and everolimus (1 or 10 nmol/L) significantly reduced the viability of the CCC cell lines (Figure 5A), with CI (as determined by the Chou-Talalay method) <1.0 in all 5 cell lines (range, 0.571-0.725; Figure 5B), indicating the synergistic effect of these 2 inhibitors. The IC_{50} values of DS-3032b or everolimus alone are summarized in Figure 5B. Moreover, combined DS-3032b (250 or 1000 nmol/L) and everolimus (15.6 nmol/L) treatment increased the sub-G_1 fraction of cells (from 41.0% to 53.2%; Figure 5C) and induced the expression of proapoptotic proteins, such as PUMA (Figure 5D). In OVISE cells, MDM2 and p53 levels were increased by DS-3032b treatment, whereas phospho-S6 and phospho-4EPB1 levels were decreased by everolimus treatment (Figure 5D). The results obtained showed both DS-3032b and everolimus targeted the signaling pathways individually.

We evaluated the in vivo antitumor activity of combined treatment using the xenograft models of OVISE, Caki-1, and ES-2 cells. The group receiving combined treatment showed a significantly smaller tumor diameter ($P < .05$) compared with that of the control group or the single-agent groups (Figure 6A-C). The mice displayed no other observable behavioral or visual changes. Additionally, TUNEL assays revealed the apoptosis-inducing ability of combined treatment, with a significant increase in TUNEL^{+} cells relative to those observed in controls (Figure 6D). Moreover, the CD31 immunohistochemistry of the xenografted tumors showed a significantly reduced number of CD31^{+} cells following combined treatment relative to that observed following treatment with either agent alone (Figure 6E).

4 | DISCUSSION

The present study examined the antitumor effects and inhibition of ascites by the combined inhibition of MDM2 and mTOR in CCOC and CCRC cells with WT *TP53*. Clear cell ovarian carcinoma was originally
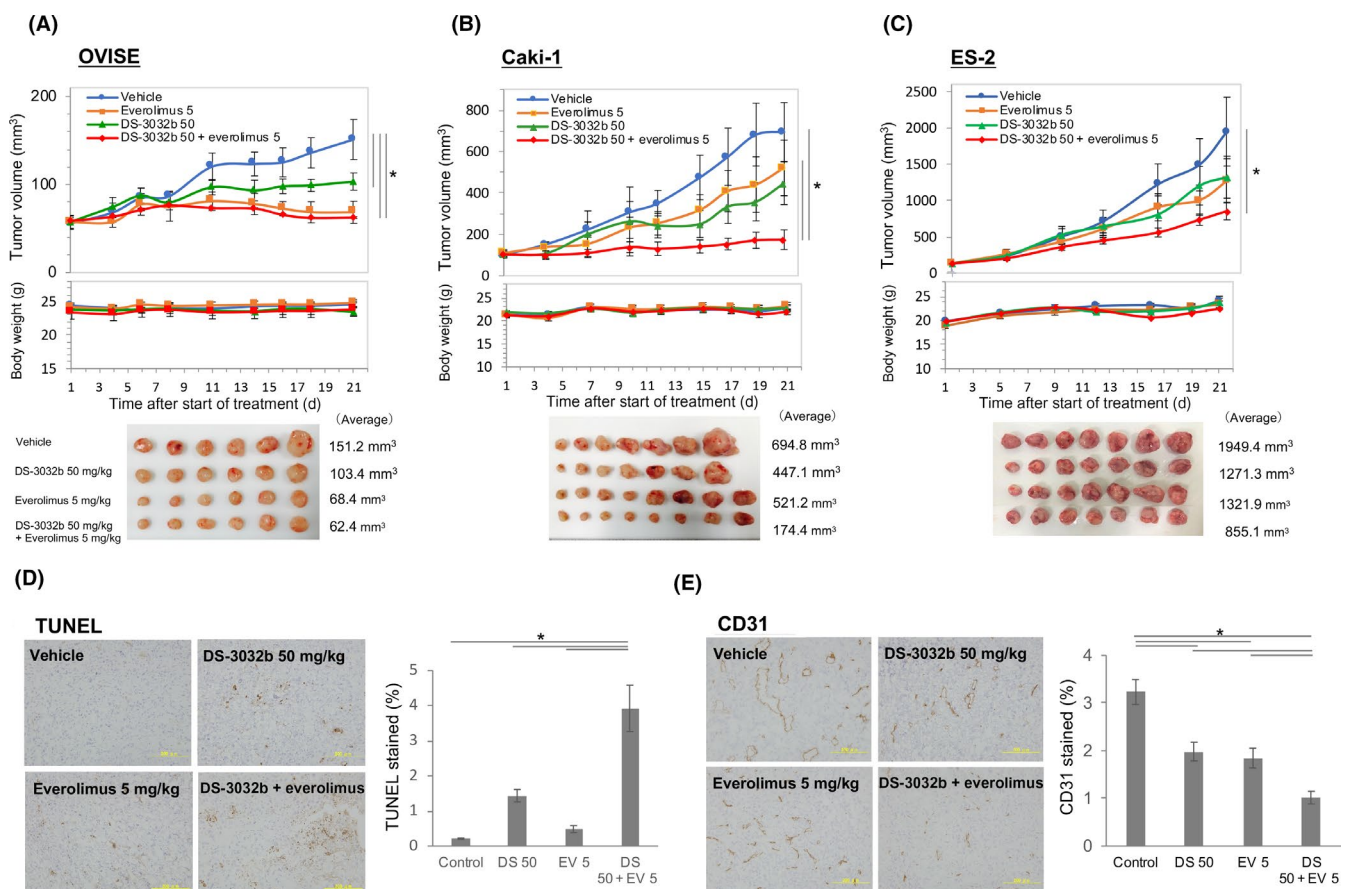

FIGURE 5 Synergic effect of combined treatment with DS-3032b and everolimus in vitro. A, After treatment with various concentrations of DS-3032b (4.9-5000 nmol/L) and everolimus (0.1, 1, and 10 nmol/L) for 72 h, 4 clear cell carcinoma (CCC) cell lines with WT *TP53* were subjected to a cell viability assay. Cell viability (%) was normalized to cells treated with 0.1% DMSO. B, IC_{50} values and the combination index for DS-3202b and everolimus in 4 CCC lines. C, Combined treatment increased the ratio of the sub-G_1 fraction in OVISE cells. OIVSE cells were treated with 250 nmol/L DS-3032b and 15.6 nmol/L everolimus or 0.1% DMSO for 4 h, and cell cycle status was analyzed by flow cytometry and propidium iodide staining. D, Expression of MDM2, p53 target proteins, and mTOR target proteins according to western blot analysis

termed mesonephroid, as it was thought to originate from the mesonephric structure and resembled renal carcinoma.[31] Therefore, CCOC and CCRC are considered developmentally and histologically similar. Unsupervised clustering assays show that the transcriptomic landscape of CCOC is closer to that of CCRC than to other ovarian and endometrial cancers.[7] However, the standard treatment regimens for these diseases are currently vastly different from one another. Patients with CCOC are conventionally treated with surgery and combination chemotherapy; however, the 3-year survival rate of these patients with residual tumors larger than 2 cm is only 10.2%.[32] Vascular invasion observed in patients with CCOC and CCRC, and specifically ascites in patients with CCOC, is particularly associated with poor disease outcomes.[33] The MET inhibitor cabozantinib shows therapeutic efficiency against CCRC but was clinically ineffective in 13 patients with recurrent CCOC.[34] Therefore, the development of a novel therapeutic strategy to improve the prognosis of CCC is warranted.

Here, we revealed the activity of MDM2 inhibitors against CCCs originating from both ovaries and kidneys and confirmed that DS-5272 showed p53-mediated inhibition of cell growth of the WT *TP53* mouse ovarian cancer cell line ID8 (Figure S2). To evaluate the direct inhibitory effect of DS-5272 on ascites production, an ID8 mouse model with cancerous ascites was created to mimic the malignant hemorrhagic ascites observed in CCCs.[35] We found that DS-5272 significantly decreases ascites volume and serum VEGF levels (Figure 3E,F), indicating p53-dependent or -independent VEGF inhibition directly through MDM2 inhibition. Although the suppression of ascites likely occurs due to multiple physical factors, our results indicated that a decrease in tumor volume reduces VEGF secretion from tumor cells. In turn, this improves peritoneal permeability and increases the reabsorption of ascites by improving lymphatic obstruction and abdominal distension. In recent years, several therapeutic agents for cancerous ascites have been developed, including: catumaxomab, a mAb against the epithelial cell-adhesion molecule; aflibercept, a VEGF target fusion protein; ramucirumab, a VEGF2 Ab; and bevacizumab, an anti-VEGF Ab. However, although known to significantly reduce ascites volume, none of these agents improved OS in clinical trials.[36] Regarding MDM2 inhibitors, previous studies reported that LQFM030 shows antitumor effects and an inhibitory effect on ascites production on Ehrlich ascites tumor cells derived from breast cancer.[37,38] Although the genetic and biological

FIGURE 6 Synergic effect of combined treatment with DS-3032b and everolimus in vivo. A-C, OVISE (A), Caki-1 (B), and ES-2 (C) cells (2 × 10^{7}) were injected s.c. into specific pathogen-free female nude mice (BALB/cAJc1-nu/nu) randomly assigned to 3 groups (n = 7-8/group) and receiving a daily oral dose of DS-3032b and/or everolimus for 3 wk. Tumor size and body weight of xenograft mouse models orally treated with DS-3032b and/or everolimus were measured after the start of DS-3032b treatment. D, Tumors were collected from mice killed after 21 d of DS-3032b and/or everolimus treatment. The number of TUNEL^{+} cells was compared with that following treatment with either agent alone. E, CD31 immunohistochemistry of the xenografted tumors. The number of CD31^{+} cells following DS-3032b and/or everolimus treatment was compared with that following treatment with either agent alone

characteristics of CCCs are becoming clear, no single specific inhibitor has been shown to be sufficiently effective.

To the best of our knowledge, this is the first preclinical study to investigate the inhibitory effect of an MDM2 inhibitor on both the suppression of ascites production and the prolongation of survival time in CCCs originating from both ovaries and kidneys. One of the most useful applications of preclinical mouse models in basic research should be to clarify therapeutic mechanisms. The preclinical models used in this study were necessary to mimic ovary and kidney CCCs with cancerous ascites in vivo. Murine double-minute 2 inhibitors are currently undergoing phase I through III clinical trials as therapeutic agents against various carcinomas, such as malignant lymphoma, leukemia, and cancers.[12,39-41] The disease-control rates of phase I studies range from 21% to 83%; however, no clinical trials of MDM2 inhibitors against both ovary and kidney CCCs have been undertaken, and as such, further development in this field is strongly desired. As shown in our previous publication, the frequency of CCOCs that have both WT _TP53_ and _MDM2_ amplification is estimated to be approximately 30% of all CCOCs. It is noteworthy that this population of CCOC patients was associated with poor prognosis.[4]

Currently, several clinical trials, including those testing the combination of everolimus and the VEGF inhibitor bevacizumab,[42,43] are targeting the PI3K/Akt/mTOR pathway. To evaluate the effectiveness of the combined inhibition of Akt/mTOR and MDM2 against CCCs, we evaluated everolimus as a concomitant drug with DS-3032b. We observed a synergistic antitumor effect of everolimus in vitro when used in combination with the MDM2 inhibitor DS-3032b (Figure 5). Moreover, both DS-3032b and everolimus independently inhibited cell growth in vivo, and these inhibitory effects appeared to work synergistically against CCCs (Figure 6).

There are several limitations to this study. First, we used cultured cell lines for preclinical models. Patient-derived xenografts from primary tumors could be superior to current models, as _MDM2_ expression varies among CCC specimens. Further investigation is needed using patient-derived xenografts to determine whether _TP53_ mutations and _MDM2_ expression are measurable biomarkers that predict MDM2 inhibitor sensitivity in CCC patients. In recent years, clinical gene panel sequencing tests have been utilized for advanced medical treatment. It is hoped that genetic testing will reveal activating mutations or amplification of _MDM2_ or PI3K/Akt/mTOR pathway genes, and if no _TP53_ mutation is found, an MDM2 and/or mTOR inhibitor could increase the antitumor effect. Indeed, of the 230 gene panel tests undertaken by the recently approved NCC Oncopanel System, we found 2 cases where an MDM2 inhibitor was used due to _MDM2_ amplification, and 1 case where an mTOR inhibitor was used due to a _PIK3CA_ mutation.[44]

Overall, our study suggests that MDM2 inhibitors potently inhibit both angiogenesis and cell growth in CCCs originating from both ovaries and kidneys. The combined use of an mTOR inhibitor significantly reinforced this effect, with no visible toxic effects, including weight loss, observed in in vivo experiments. Further studies targeting the disruption of _TP53-MDM2_ binding, including the characterization of effective concentrations, are required before proceeding to clinical trials that target advanced CCCs in patients with massive ascites.

CONFLICT OF INTEREST

KO received a research grant from Daiichi-Sankyo and lecture fees from Chugai Pharmaceutical and AstraZeneca. KN received a research grant and lecture fee from MSD. The other authors declare that they have no conflicts of interest.

ORCID

Kazunori Nagasaka https://orcid.org/0000-0002-0696-5175

REFERENCES

1. Wade M, Li YC, Wahl GM. MDM2, MDMX and p53 in oncogenesis and cancer therapy. _Nat Rev Cancer_. 2013;13:83-96.
2. Momand J, Jung D, Wilczynski S, et al. The MDM2 gene amplification database. _Nucleic Acids Res_. 1998;26:3453-3459.
3. Moll UM, Petrenko O. The MDM2-p53 interaction. _Mol Cancer Res_. 2003;1:1001-1008.
4. Makii C, Ikeda Y, Oda K, et al. Anti-tumor activity of dual inhibition of phosphatidylinositol 3-kinase and MDM2 against clear cell ovarian carcinoma. _Gynecol Oncol_. 2019;155:331-339.
5. Sugiyama T, Kamura T, Kigawa J, et al. Clinical characteristics of clear cell carcinoma of the ovary: a distinct histologic type with poor prognosis and resistance to platinum-based chemotherapy. _Cancer_. 2000;88:2584-2589.
6. Itamochi H, Kigawa J, Terakawa N. Mechanisms of chemoresistance and poor prognosis in ovarian clear cell carcinoma. _Cancer Sci_. 2008;99:653-658.
7. Ji JX, Wang YK, Cochrane DR, et al. Clear cell carcinomas of the ovary and kidney: clarity through genomics. _J Pathol_. 2018;244:550-564.
8. Haitel A, Wiener HG, Baethge U, et al. mdm2 expression as a prognostic indicator in clear cell renal cell carcinoma: comparison with p53 overexpression and clinicopathological parameters. _Clin Cancer Res_. 2000;6:1840-1844.
9. Noon AP, Vlatković N, Polański R, et al. p53 and MDM2 in renal cell carcinoma: biomarkers for disease progression and future therapeutic targets? _Cancer_. 2010;116:780-790.
10. Nag S, Zhang X, Srivenugopal KS, et al. Targeting MDM2-p53 interaction for cancer therapy: are we there yet? _Curr Med Chem_. 2014;21:553-574.
11. Yang J-Y, Zong CS, Xia W, et al. MDM2 promotes cell motility and invasiveness by regulating E-cadherin degradation. _Mol Cell Biol_. 2006;26:7269-7282.
12. Rafał R, Jakub W, Joanna JA. MDM2-p53 interaction inhibitors: current state of art and updated patent review (2010-present). _Recent Pat Anticancer Drug Discov_. 2019;14:324-369.

13. Zhao Y, Aguilar A, Bernard D, Wang S. Small-molecule inhibitors of the MDM2-p53 protein-protein interaction (MDM2 Inhibitors) in clinical trials for cancer treatment. *J Med Chem*. 2015;58:1038-1052.

14. Makii C, Oda K, Ikeda Y, et al. MDM2 is a potential therapeutic target and prognostic factor for ovarian clear cell carcinomas with wild-type TP53. *Oncotarget*. 2016;7:75328-75338.

15. Patterson DM, Gao D, Trahan DN, et al. Effect of MDM2 and vascular endothelial growth factor inhibition on tumor angiogenesis and metastasis in neuroblastoma. *Angiogenesis*. 2011;14:255-266.

16. Ravi R, Mookerjee B, Bhujwalla ZM, et al. Regulation of tumor angiogenesis by p53-induced degradation of hypoxia-inducible factor 1alpha. *Genes Dev*. 2000;14:34-44.

17. Tan DSP, Agarwal R, Kaye SB. Mechanisms of transcoelomic metastasis in ovarian cancer. *Lancet Oncol*. 2006;7:925-934.

18. Samuels Y, Wang Z, Bardelli A, et al. High frequency of mutations of the PIK3CA gene in human cancers. *Science*. 2004;304:554.

19. Kashiyama T, Oda K, Ikeda Y, et al. Antitumor activity and induction of TP53-dependent apoptosis toward ovarian clear cell adenocarcinoma by the dual PI3K/mTOR inhibitor DS-7423. *PLoS One*. 2014;9:e87220.

20. Oda K, Hamanishi J, Matsuo K, et al. Genomics to immunotherapy of ovarian clear cell carcinoma: Unique opportunities for management. *Gynecol Oncol*. 2018;151:381-389.

21. Kuo K-T, Mao T-L, Jones S, et al. Frequent activating mutations of PIK3CA in ovarian clear cell carcinoma. *Am J Pathol*. 2009;174:1597-1601.

22. Mabuchi S, Sugiyama T, Kimura T. Clear cell carcinoma of the ovary: molecular insights and future therapeutic perspectives. *J Gynecol Oncol*. 2016;27:e31.

23. Yuan TL, Cantley LC. PI3K pathway alterations in cancer: variations on a theme. *Oncogene*. 2008;27:5497-5510.

24. Janku F, Yap TA, Meric-Bernstam F. Targeting the PI3K pathway in cancer: are we making headway? *Nat Rev Clin Oncol*. 2018;15(5):273–291.

25. Gottlieb TM, Leal JFM, Seger R, et al. Cross-talk between Akt, p53 and Mdm2: possible implications for the regulation of apoptosis. *Oncogene*. 2002;21:1299-1303.

26. Stambolic V, MacPherson D, Sas D, et al. Regulation of PTEN transcription by p53. *Mol Cell*. 2001;8:317-325.

27. Shih-Chu Ho E, Lai C-R, Hsieh Y-T, et al. p53 mutation is infrequent in clear cell carcinoma of the ovary. *Gynecol Oncol*. 2001;80:189-193.

28. Amano T, Chano T, Yoshino F, et al. Current position of the molecular therapeutic targets for ovarian clear cell carcinoma: a literature review. *Healthcare (Basel)*. 2019;7:E94.

29. Miyazaki M, Uoto K, Sugimoto Y, et al. Discovery of DS-5272 as a promising candidate: A potent and orally active p53-MDM2 interaction inhibitor. *Bioorg Med Chem*. 2015;23:2360-2367.

30. Arnhold V, Schmelz K, Proba J, et al. Reactivating TP53 signalling by the novel MDM2 inhibitor DS-3032b as a therapeutic option for high-risk neuroblastoma. *Oncotarget*. 2018;9:2304-2319

31. Eastwood J. Mesonephroid (clear cell) carcinoma of the ovary and endometrium: a comparative prospective clinico-pathological study and review of literature. *Cancer*. 1978;41:1911-1928.

32. Shu CA, Zhou Q, Jotwani AR, et al. Ovarian clear cell carcinoma, outcomes by stage: the MSK experience. *Gynecol Oncol*. 2015;139:236-241.

33. Takano M, Kikuchi Y, Yaegashi N, et al. Clear cell carcinoma of the ovary: a retrospective multicentre experience of 254 patients with complete surgical staging. *Br J Cancer*. 2006;94:1369-1374.

34. Konstantinopoulos PA, Brady WE, Farley J, et al. Phase II study of single-agent cabozantinib in patients with recurrent clear cell ovarian, primary peritoneal or fallopian tube cancer (NRG-GY001). *Gynecol Oncol*. 2018;150:9-13.

35. Roby KF, Taylor CC, Sweetwood JP, et al. Development of a syngeneic mouse model for events related to ovarian cancer. *Carcinogenesis*. 2000;21:585-591.

36. Smolle E, Taucher V, Haybaeck J. Malignant ascites in ovarian cancer and the role of targeted therapeutics. *Anticancer Res*. 2014;34:1553-1561.

37. da Mota MF, Cortez AP, Benfica PL, et al. Induction of apoptosis in Ehrlich ascites tumor cells via p53 activation by a novel small-molecule MDM2 inhibitor - LQFM030. *J Pharm Pharmacol*. 2016;68:1143-1159.

38. da Mota MF, de Carvalho FS, de Ávila RI, et al. LQFM030 reduced Ehrlich ascites tumor cell proliferation and VEGF levels. *Life Sci*. 2018;201:1-8.

39. Andreeff M, Kelly KR, Yee K, et al. Results of the phase I trial of RG7112, a small-molecule MDM2 antagonist in leukemia. *Clin Cancer Res*. 2016;22:868-876.

40. Ray-Coquard I, Blay J-Y, Italiano A, et al. Effect of the MDM2 antagonist RG7112 on the P53 pathway in patients with MDM2-amplified, well-differentiated or dedifferentiated liposarcoma: an exploratory proof-of-mechanism study. *Lancet Oncol*. 2012;13:1133-1140.

41. Wagner AJ, Banerji U, Mahipal A, et al. Phase I Trial of the human double minute 2 inhibitor MK-8242 in patients with advanced solid tumors. *J Clin Oncol*. 2017;35:1304-1311.

42. Tew WP, Sill MW, Walker JL, et al. Randomized phase II trial of bevacizumab plus everolimus versus bevacizumab alone for recurrent or persistent ovarian, fallopian tube or peritoneal carcinoma: An NRG oncology/gynecologic oncology group study. *Gynecol Oncol*. 2018;151:257-263.

43. Taylor SE, Chu T, Elvin JA, et al. Phase II study of everolimus and bevacizumab in recurrent ovarian, peritoneal, and fallopian tube cancer. *Gynecol Oncol*. 2020;156:32-37.

44. Sunami K, Ichikawa H, Kubo T, et al. Feasibility and utility of a panel testing for 114 cancer-associated genes in a clinical setting: A hospital-based study. *Cancer Sci*. 2019;110:1480-1490.

SUPPORTING INFORMATION

Additional supporting information may be found online in the Supporting Information section.